Precision Agric (2015) 16:532–557
DOI 10.1007/s11119-015-9393-x

Integrating geospatial data and cropping system simulation within a geographic information system to analyze spatial seed cotton yield, water use, and irrigation requirements

K. R. Thorp[1] · D. J. Hunsaker[1] · A. N. French[1] · E. Bautista[1] · K. F. Bronson[1]

Published online: 14 April 2015

Abstract The development of sensors that provide geospatial information on crop and soil conditions has been a primary success for precision agriculture. However, further developments are needed to integrate geospatial data into computer algorithms that spatially optimize crop production while considering potential environmental impacts and resource limitations. The objective of this research was to combine several information technologies, including remote sensing, a cropping system model, and a geographic information system (GIS), to synthesize and interpret geospatial data collected during two irrigation scheduling experiments conducted in 2009 and 2011 in a 5-ha cotton field in central Arizona. The Geospatial Simulation (GeoSim) plug-in for Quantum GIS was used to manage geospatial data and conduct site-specific simulations with the CSM-CROPGRO-Cotton model. Simulated annealing optimization was used to adjust five model parameters to simulate site-specific conditions in 320 zones across the field. Using input parameters for GeoSim, a multiple criteria objective function was developed to incorporate measured and simulated leaf area index (LAI), crop canopy height, seed cotton yield, and evapotranspiration (ET) for site-specific optimization of CSM-CROPGRO-Cotton. Parameter identifiability and equifinality issues associated with model inversion were investigated. The optimized model was used for post hoc analysis of irrigation rates that maximized site-specific irrigation water use efficiency. With spatial optimization, the model was able to simulate LAI with root mean squared errors (RMSE) of 15 and 8 % in the 2009 and 2011 experiments, respectively. The RMSEs between measured and simulated canopy height, seed cotton yield, and ET were 5 % or less in both seasons. Some parameters were more identifiable than others during model inversions. Multiple temporal estimates of LAI were effective for constraining the model's specific leaf area parameter (SLAVR, $cm^2\ g^{-1}$), but lack of information on root growth reduce identifiability of a parameter related to that process (SRGF0). Post-hoc simulation analysis of irrigation management options showed that irrigation schedules based on remotely sensed vegetation indices increased irrigation

✉ K. R. Thorp
kelly.thorp@ars.usda.gov

[1] USDA-ARS, Arid-Land Agricultural Research Center, Maricopa, AZ, USA

water use efficiency as compared to traditional scheduling methods, particularly in the 2009 growing season. In 2011, the analysis showed that all scheduling methods resulted in excess irrigation application, and higher deep seepage rates were simulated in that season. Taken together, the results demonstrate that well-designed software tools and algorithms for data processing and interpretation can be potentially transformative for integrating multiple geospatial data sets to compute optimum scenarios for precision irrigation management.

Keywords Crop model · Height · Inverse modeling · Leaf area index · Model inversion · Optimization · Precision agriculture · Remote sensing · Simulated annealing · Yield

Introduction

Concerns about water scarcity, arising due to aridity, drought, desertification, and water shortage, have driven efforts to improve approaches for managing agricultural irrigation water (Pereira et al. 2002). Precision irrigation technologies, which aim to apply the appropriate amount of water at the appropriate place and time, have emerged as a viable solution for optimizing crop production under water resource constraints (Monaghan et al. 2013). Engineering solutions for precision irrigation management have led to control systems on mechanical move irrigation machines capable of applying water on a site-specific basis (Camp et al. 1998; Kranz et al. 2012). Further improvements have permitted remote monitoring of the irrigation system through the Internet and integration of wireless sensor networks that provide real-time information on soil moisture and meteorological conditions (Chávez et al. 2010). Dynamic models of crop growth and soil water balance have also been incorporated into irrigation control systems for development, evaluation, and implementation of precision irrigation strategies in real-time (McCarthy et al. 2010). However, management decisions that optimize irrigation schedules and improve water use efficiency remain complex and are dependent on multiple factors: crop status, soil conditions, meteorology, commodity prices, water resource constraints, and others. Continued efforts are needed to develop computer algorithms and decision support systems that holistically combine information from multiple sources to calculate and implement spatially and temporally optimized irrigation strategies (Evans and King 2012).

Cropping system simulation models can serve as the central computational component of decision support systems for precision irrigation. Such models combine information on meteorological conditions, soil characteristics, crop cultivars, and management practices to simulate hydrology, nutrient dynamics, and crop growth and development processes on daily or hourly time steps (e.g., Thorp et al. 2014a). Since simulating crop growth responses to root-zone soil moisture shortages is a primary function of cropping system models, they have been regularly used in research to evaluate irrigation management options (Baumhardt et al. 2009; Hood et al. 1987; Hook 1994) and to assess the economics of irrigation management decisions (Cammarano et al. 2012; Mauget et al. 2013). Nair et al. (2013) used the Cotton2K model to assess cotton (*Gossypium hirsutum* L.) productivity and profitability when water resource constraints permitted irrigating only a subset of the total field area. DeJonge et al. (2007) used CERES-Maize to analyze the potential for precision irrigation to improve maize (*Zea mays* L.) yields and revenue in Iowa. Current limitations of cropping system models for applications in precision irrigation

include (1) the typical design characteristic of simulating conditions at one point on the landscape and (2) the large parameterization requirements for model implementation at multiple spatial locations.

To overcome the point-based design limitation of cropping system models, a geographic information system (GIS) can offer functionality for conducting model simulations spatially. A GIS can facilitate mapping, visualization, and geoprocessing of spatial data within unique geospatial units across a field. Several modern GIS packages also provide access to their application programming interface (API) and support scripting languages, which permit savvy GIS technicians to develop custom plug-ins that automate geoprocessing and data management tasks. This functionality of GIS software has been used to develop links to cropping system models and to conduct spatial simulations for addressing diverse topics in precision agriculture. For example, Rao et al. (2000) linked the Erosion Productivity Impact Calculator (EPIC) model with a GIS and simulated site-specific nitrogen dynamics under conventional and minimum tillage over a 5-year period at a field site in Oklahoma. McKinion et al. (2001) integrated the GOSSYM model with a GIS to analyze precision irrigation and nitrogen fertilization prescriptions. With spatial optimization of water and nitrogen management, GOSSYM simulated a 322 kg ha^{-1} increase in cotton yield with a 2.6 cm ha^{-1} increase in irrigation and a 35 kg ha^{-1} decrease in nitrogen fertilizer. Thorp et al. (2008) developed the Apollo decision support software, which conducted simulations for site-specific crop model calibration and evaluation (Thorp et al. 2007) and analysis of precision nitrogen (Thorp et al. 2006) and irrigation (DeJonge et al. 2007) management options. Separate GIS algorithms were developed to prepare the model input files required for spatial simulations in Apollo. More recently, Thorp and Bronson (2013) developed an open-source GIS tool that could manage spatial simulations for any point-based cropping system model. They demonstrated the tool using both the AquaCrop and CSM-CROPGRO-Cotton models to simulate site-specific seed cotton (fiber + seed) yield in response to irrigation management, nitrogen management, and soil texture variability for a 14 ha study area near Lamesa, Texas. Others have linked cropping system models with GIS for analyses of crop yield and water use relationships at regional scales (Heinemann et al. 2002; Ines et al. 2002; Liu 2009).

To assist parameterization of cropping system models for spatial simulations or to provide data for updating model state variables spatially, remote sensing technologies have been used to rapidly quantify spatial variability in crop canopy characteristics. For example, Seidl et al. (2004) computed the normalized difference vegetation index (NDVI) from airborne remote sensing imagery and used the index to update the leaf weight state variable in spatial simulations with the CROPGRO-Soybean model. The updating procedure improved coefficients of determination (r^2) between measured and simulated soybean (*Glycine max* (L.) Merr.) yield in some fields, but improvements were dependent on the timing of remote sensing reconnaissance. Several studies have similarly used ground-based NDVI measurements to estimate leaf area index (LAI) and test impacts of updating simulated LAI or related leaf growth state variables on simulated evapotranspiration (ET) and crop yield (Hadria et al. 2006; Thorp et al. 2010). El Nahry et al. (2011) described efforts to combine Landsat remote sensing imagery, the Surface Energy Balance Algorithm for Land (SEBAL) model for instantaneous ET calculations, the FAO Cropwat model for Penman–Monteith daily time-series ET calculations, and maps of yield and soil variability within a GIS for analysis of the economic and environmental impacts of precision irrigation and nitrogen fertilization. Although costs of applying precision management were much greater than traditional practices, their analysis demonstrated economic benefits with the former approach due to increased crop yields. Integration of remote sensing data and

crop growth simulations within a GIS has also occurred at regional scales (Ju et al. 2010; Mo et al. 2005). These studies demonstrate the utility of combining multiple informational tools for analyzing spatial variability in crop yield, ET, and other important cropping system variables.

Multiple approaches are available for combining data from remote sensing imagers and other sensors into the simulations of cropping system models. A common technique uses model inversion for adjusting parameters to minimize error between measured and simulated data. For example, Calmon et al. (1999) used simulated annealing optimization to adjust soil and root growth parameters in CROPGRO-Soybean to minimize error between measured and simulated volumetric soil moisture content. Model inversion has been regularly used in precision agriculture research to estimate soil hydraulic properties and other factors that govern site-specific yield variability (Irmak et al. 2001; Paz et al. 1998; Thorp et al. 2007). Charoenhirunyingyos et al. (2011) used estimates of LAI and ET from Moderate Resolution Imaging Spectrometer (MODIS) data to estimate soil hydraulic parameters in the Soil Water Atmosphere Plant (SWAP) model, which improved soil moisture simulations to a depth of 28 cm. An important feature of their study was the use of multiple criteria objective functions to solve the inverse problem for multiple variables. Thorp et al. (2012) linked two radiative transfer models with a cropping system model and used optimization to adjust leaf area growth parameters to minimize error between measured and simulated NDVI or canopy spectral reflectance. As compared to stand-alone simulations, estimates of wheat (*Triticum durum* L.) yield and LAI were improved using remote sensing data to optimize the coupled models. Model inversion was also used to estimate dual crop coefficients using FAO-56 ET methods and measured soil water potential (Zhang et al. 2011) .

The overall objective of this research was to combine several information technologies, including remote sensing, a cropping system model, and GIS, to synthesize and interpret geospatial data collected during two irrigation scheduling experiments in a 5-ha cotton field in central Arizona. Specific objectives were to (1) use the Geospatial Simulation plug-in for Quantum GIS (Thorp and Bronson 2013) to manage geospatial data within site-specific harvest zones and conduct spatial simulations with a cotton model, (2) develop and evaluate an optimization approach that used measured NDVI, crop height, soil moisture, and yield to estimate five model parameters and calibrate the model for site-specific conditions, and (3) use the calibrated model to evaluate the irrigation scheduling approaches tested in the experiment by assessing their ability to maximize site-specific irrigation water use efficiency.

Materials and methods

Field experiments

As described by Hunsaker et al. (2015), irrigation scheduling experiments were conducted in a 5-ha cotton field from May to October in 2009 and 2011 at the University of Arizona's Maricopa Agricultural Center (MAC) near Maricopa, Arizona (33.075°N, 111.990°W, 361 m above sea level). Soils at the site were a mixture of Casa Grande sandy loam (fine-loamy, mixed, hyperthermic, Typic Natrargids) to the east and Trix clay loam (fine-loamy, mixed calcareous, hyperthermic Typic Torrifluvents) to the west. The environment at MAC is arid with maximum daily air temperatures regularly exceeding 38 °C in July and August.

Precipitation amounted to 68 and 24 mm during the 2009 and 2011 cotton growing seasons, respectively.

Sixteen treatment plots were established with a north–south orientation, each hydrologically isolated with border dikes and containing 12 cotton rows with spacing of 1.0 m and length of 168 m (Fig. 1). Upland cotton (cv. 'Deltapine 1044B2RF') was planted in raised beds on 22 April 2009 [day of year (DOY) 112] and 20 April 2011 (DOY 110). Average post-emergence plant densities were 22.0 plants m^{-2} in 2009 and 15.2 plants m^{-2} in 2011. Four replicates of four experimental treatments were randomized in a complete block design to test four methodologies for irrigation scheduling. The 'MAC' treatment imitated irrigation scheduling practices of the MAC farm supervisor who managed adjacent cotton fields and used visual assessments of crop stress and personal experience to make irrigation management decisions. The 'FAO' treatment used FAO-56 methods (Allen et al. 1998) with site-specific soil texture data and a soil water balance model to schedule irrigations when available root zone soil moisture was depleted to 45 % of total available capacity. The 'VI_A' treatment was identical to FAO, except remotely sensed NDVI was used to estimate site-specific crop coefficients for FAO-56 ET calculations. The 'VI_B' treatment was identical to VI_A, except irrigations were scheduled when available root zone soil moisture in 5 % of the treatment area was depleted to 65 % of total available capacity.

No mechanical move irrigation systems were available on-farm at the time of these studies, which limited the potential for true precision irrigation. Water for surface irrigation was delivered through gated polypipe, which was hard-plumbed to a concrete-lined irrigation ditch on the southern side of the field. Treatment plots were irrigated individually, and irrigation volumes applied to each plot were monitored with an in-line propeller flow meter. Nine irrigation events occurred for each treatment plot in each growing season, but the irrigation rates and dates varied. Since surface irrigation leads to variable opportunity time for infiltration which contributes to spatially variable infiltration rates (Hunsaker et al.

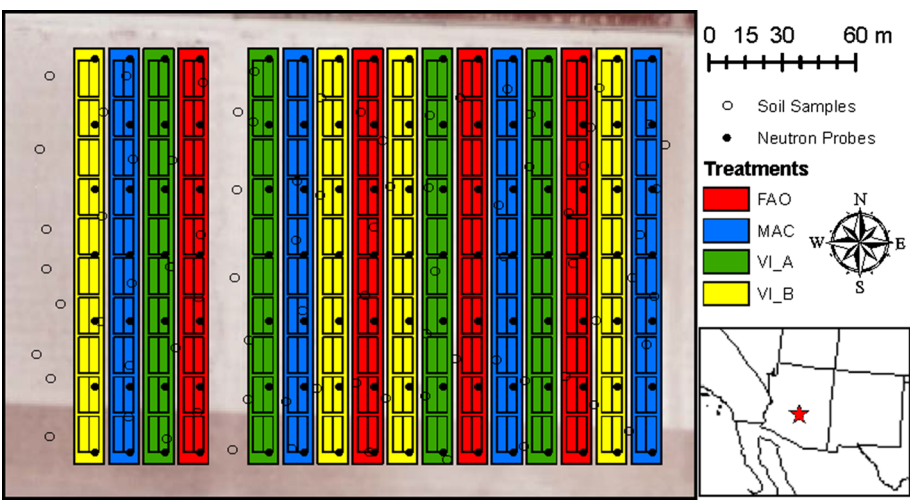

Fig. 1 Field map of irrigation treatments for the 2009 and 2011 cotton field experiments in Maricopa, Arizona with locations of random soil samples and access tubes for neutron probes. Twenty zones for site-specific cotton harvest were delineated within each irrigation treatment (Color figure online)

1999; Jaynes and Hunsaker 1989), seven water sensor timers, manufactured in-house (Hunsaker et al. 2011), were positioned in the furrow adjacent to the neutron access tube locations. The sensors recorded the time that water arrived (advance time) and the time that water had completely receded below the soil surface (recession time). Information on irrigation flow rate, furrow geometry, and advance and recession times were used within the WinSRFR simulation software (Bautista et al. 2009) to estimate site-specific irrigation infiltration at the location of each neutron access tube.

Pre-season soil profile nitrate was adequate in both seasons, so no pre-plant nitrogen fertilizer was applied in either year. Based on analyses of cotton petiole nitrate concentration, 56 kg nitrogen ha^{-1}, as liquid urea-ammonium-nitrate, was uniformly applied to all treatments on 1 June 2009 (DOY 152) and 31 May 2011 (DOY 151).

Site-specific ground measurements

Access tubes for neutron moisture meters were installed at 112 locations in both seasons. Seven tubes were installed 25 m apart along one cotton row in each treatment plot (Fig. 1). Field-calibrated neutron moisture meters (Model 503, Campbell Pacific Nuclear, CPN, Martinez, California) were used to measure the soil water contents from 0.1 to 2.9 m in 0.2 m incremental depths. During each cotton experiment, soil water content was measured at each location approximately 21 times from mid-May to mid-September. Measurements were typically made 1 day before irrigating a treatment plot and again 4 or 5 days after the irrigation. Soil water content data were used to estimate ET and deep seepage between successive measurement events at each location using the soil water balance approach described by Hunsaker et al. (2005):

$$\mathrm{ET} = \sum_{i=1}^{11}\left(D_{i,1} - D_{i,n-1}\right) + \sum_{j=1}^{n-1}\left(R_j + I_j\right) - \mathrm{DS} \tag{1}$$

$$\mathrm{DS} = \sum_{i=12}^{15}\left(D_{i,1} - D_{i,n-1}\right) \tag{2}$$

where ET is the total evapotranspiration and DS is the total deep seepage occurring from day 1 to the end of day n–1, $D_{i,1}$ and $D_{i,n\text{-}1}$ are respectively the water depth measurements at soil depth increment i at the beginning of day 1 and end of day n–1, and R_j and I_j are respectively the precipitation and irrigation depths received on day j. Equation 1 was used with DS equal to zero if Eq. 2 resulted in DS less than zero. Soil depth increments 1 through 11 were used to estimate the change in soil water storage and corresponded to actual soil depths of 10–210 cm. Soil depth increments 12 through 15 were used to estimate deep seepage and corresponded to actual soil depths of 230 to 290 cm.

During the installation of neutron access tubes in 2009, soil samples in 0.3 m increments to a depth of 1.8 m were collected from the 112 bore holes. Prior to the 2011 experiment, additional soil cores were collected at 80 random locations across the field (Fig. 1). To quantify soil texture, samples were analyzed for particle size fraction in the laboratory using the Bouyoucos hydrometer method (Gee and Bauder 1986). The Rosetta pedotransfer functions (Schaap et al. 2001) were used to calculate soil bulk density, saturated hydraulic conductivity, and soil water limits, including the saturated soil water content (porosity), drained upper limit (field capacity), and lower limit (wilting point) based on soil texture data at each depth and location.

Cotton plant height was regularly measured near the second, fourth, and sixth neutron access locations in each treatment plot. In 2009, plant height was measured 6 times from 3 June (DOY 154) through 7 August (DOY 219). In 2011, height was measured 14 times from 10 May (DOY 130) through 19 August (DOY 231).

Twenty zones were delineated in each treatment plot for site-specific cotton yield measurements, each four rows by 16 m (Fig. 1). Within each zone, cotton was machine-harvested with a two-row picker from 23 to 28 October in 2009 (DOY 296–301) and from 11 to 14 October in 2011 (DOY 284–287). Two passes were required to harvest cotton in each zone. Samples from each pass were bagged and weighed separately in the field. Later, subsamples from each bag were weighed and ginned. Fiber turnout percentages were used to correct the original bulk cotton weights to fiber and seed weights. Based on limited measurements, fiber and seed weights were further reduced by 3.5 and 4.9 %, respectively, to account for moisture. Seed cotton yield in each harvest zone was computed as the sum of the corrected fiber and seed weights from the appropriate neighboring harvest swaths divided by the zone area (58.8 m^2).

Airborne remote sensing

As described by French et al. (2015), airborne remote sensing surveys were conducted over the field site on multiple occasions in 2009 and 2011. The present study required only NDVI measurements from multispectral cameras sensitive in the visible and near-infrared (NIR) spectrum; however, a thermal infrared camera was also routinely deployed for surface temperature measurements. In 2009, a 3-band multispectral camera (MS3100, DuncanTech, Auburn, California) was deployed for NDVI measurements. After an electronic failure, the DuncanTech camera was replaced for the 2011 season: first with a pair of 8-bit machine vision cameras (EO-1312M, Edmund Optics, Barrington, New Jersey) and later with a new 3-band multispectral camera (MS4100, Geospatial Systems, Inc., Rochester, New York). Cameras were mounted on an aluminum plate, attached to the frame of a Hiller UH-12 helicopter, and flown approximately 800 m above ground level, which provided images with spatial resolution of approximately 0.25 m. Red and NIR image data for NDVI calculations were collected using 10 nm bandwidth filters centered at 670 and 790 nm. The present analysis used images acquired on 3 June (DOY 154) and 30 July (DOY 211) in 2009. Images from five collection dates in 2011 were used: 26 May (DOY 146), 9 June (DOY 160), 21 July (DOY 202), 4 August (DOY 216), and 18 August (DOY 230).

On the morning of remote sensing surveys, four 8 m by 8 m calibration tarps (Group VIII Technologies, Provo, Utah) were positioned near the cotton field. Concurrently with airborne image acquisition, ground-based radiometric measurements of each calibration tarp were collected with a portable field spectroradiometer (GER1500, Spectra Vista Corporation, Poughkeepsie, New York). Additional radiometric measurements over a calibrated, 99 % Spectralon panel (Labsphere, Inc., North Sutton, New Hampshire) were used to characterize incoming solar irradiance and to calculate reflectance factors in the red and NIR wavebands for each calibration tarp. Using an empirical line calibration method, remote sensing images were calibrated to percent reflectance by matching the ground-based tarp reflectance data with the image digital numbers (DNs) from tarp pixels. Images were georeferenced by selecting ground control points from an orthophoto provided by the United States Geological Survey (USGS). An NDVI image on each acquisition date was calculated using the following equation:

$$\mathrm{NDVI} = \frac{\rho_{790} - \rho_{670}}{\rho_{790} + \rho_{670}} \quad (3)$$

where ρ_{790} and ρ_{670} are reflectance in the NIR and red wavebands, respectively. Image processing tasks were completed using the Environment for Visualizing Images (ENVI) software. (Version 4.8, Exelis Visual Information Solutions, Boulder, Colorado).

Geospatial data processing

Thorp and Bronson (2013) described the Geospatial Simulation plug-in for Quantum GIS (www.qgis.org), which was used to manage geospatial data and conduct site-specific cropping system model simulations in the present study. To use the tool, a 'base layer' polygon shapefile was created to delineate the spatial zones for site-specific modeling and to contain the geospatial data for each zone. The ploygon shapefile delineating the 320 zones for site-specific cotton harvest was used as the base layer shapefile for site-specific simulations (Fig. 1). Estimates of each soil hydraulic property at each sampling depth were combined with their respective geographic coordinates and represented as a point shapefiles. Universal kriging interpolation based on 20 nearest neighboring points was used to estimate the spatial distribution of each soil hydraulic property at each sampling depth on a 0.5 m grid across the field. A geoprocessing script within the Geospatial Simulation tool was used to average the soil hydraulic property estimates within each of the 320 simulation zones and append the data to the base layer attribute table. Initial soil moisture conditions in each simulation zone were specified from the nearest neutron moisture meter reading on the first measurement outing in each growing season. Likewise, the site-specific irrigation rates and the ET and deep seepage estimates at each neutron access location were assigned to the nearest simulation zones in each treatment plot. These data, along with the variable irrigation dates, were appended to the base layer shapefile for use in site-specific simulations.

Similar to the kriged maps of soil hydraulic properties, the NDVI measurements in each remote sensing image were averaged within the 320 simulation zones and appended to the base layer shapefile. Canopy height measurements at the neutron access locations were assigned to the nearest simulation zones. These NDVI and canopy height measurements were combined to estimate site-specific cotton LAI on each remote sensing image acquisition date. Using the approach of Scotford and Miller (2004), a compound canopy index (CCI) was calculated and used to estimate LAI:

$$\mathrm{LAI} = \beta * \mathrm{CCI} = \beta * \left(\frac{\mathrm{C}}{\mathrm{C_{max}}}\right) * \left(\frac{\mathrm{H}}{\mathrm{H_{max}}}\right) \quad (4)$$

where β is a regression constant, C and H are respectively the instantaneous canopy cover and height measurements, and C_{max} and H_{max} are respectively the maximum cover and height expected during the growing season. Co-located data to parameterize this calculation were collected during a subsequent cotton study at MAC during the 2013 growing season. Canopy width and height was measured at several locations on ten occasions during the period of rapid LAI expansion: 18 June (DOY 169) to 29 August (DOY 241). Overhead digital images from a height of 2 m were collected to quantify canopy cover, and measurements with an LAI meter (LAI-2200, Li-Cor, Lincoln, Nebraska) were also collected. Biomass from two 0.5-m lengths of row was destructively sampled and dissected to remove all leaves. Total leaf area of each sample was measured with an area meter (LAI-3100, Li-Cor, Lincoln, Nebraska) and used to calculate a second LAI estimate. Analysis of

these data led to values of 5.5, 87.9 %, and 110.5 cm for β, C_{max}, and H_{max}, respectively. These parameters were used for site-specific LAI calculations with the 2009 and 2011 NDVI and canopy height data. The NDVI data were used as a direct estimate of canopy cover. Using data from 2013 to estimate LAI for 2009 and 2011 was not considered problematic, because the same cotton cultivar was used for all field studies.

To complete preparation of the base layer shapefile, the seed cotton yield measured in each harvest zone was appended to the attribute table. Additional attributes were added for model input parameters requiring site-specific adjustments and for select model outputs. In summary, site-specific soil properties, initial soil water content, irrigation management data, and estimates of ET, deep seepage, canopy height, LAI, and seed cotton yield were compiled within the base layer shapefile for parameterization, evaluation, optimization, and application of the CSM-CROPGRO-Cotton model on a site-specific basis.

CSM-CROPGRO-cotton

The Decision Support System for Agrotechnology Transfer (DSSAT) Cropping System Model (CSM; ver. 4.5.1.005; Hoogenboom et al. 2012; Jones et al. 2003) utilizes mass balance principles to simulate the carbon, nitrogen, and hydrologic processes and transformations that occur within a cropping system. Processes are calculated within a homogeneous area on a daily time step, and certain subprocesses are computed hourly. With CSM-CROPGRO-Cotton, simulations of cotton development proceed through a series of stages based on photothermal unit accumulation from planting to harvest, including emergence, first leaf, first flower, first seed, first cracked boll (physiological maturity), and 90 % open boll. Light interception is simulated based on a hedgerow canopy, where the plant canopy envelope is elliptical and defined by simulated canopy height and width (Boote and Pickering 1994). Potential carbon assimilation is computed from leaf-level biochemistry based on the model of Farquhar et al. (1980), and deductions for growth and maintenance respiration are calculated explicitly. The model calculates stress effects from deficit soil water and soil nitrogen conditions, which further reduce the carbohydrate available for plant growth. Assimilated carbon is partitioned to various plant parts, including leaves, stems, roots, bolls, and seed cotton.

Simulated plant growth responds to management practices, cultivar selection, soil properties, and meteorological conditions. Management inputs required for model simulations include plant population; row spacing; seed depth; planting dates; dates and amounts of irrigation; dates, amounts, and type of fertilizer application; and dates, depths, and type of tillage. These inputs were specified as recorded during the field experiments. Cultivar parameters define day length sensitivity, heat units needed to progress through developmental stages, maximum single leaf photosynthetic rate, single leaf size, specific leaf area, maximum partitioning to bolls, individual seed size, threshing percentage, and oil and protein composition of seeds. Many of these parameters were specified based on the results of Thorp et al. (2014b), who performed the first evaluation of CSM-CROPGRO-Cotton for the central Arizona environment. Soil profiles are defined by soil water limits, root growth factors, saturated hydraulic conductivity, bulk density, pH, and initial conditions for water, inorganic nitrogen, and organic carbon. Many of these soil profile parameters were specified using site-specific data through the Geospatial Simulation tool in Quantum GIS. Required meteorological data include daily inputs for minimum and maximum temperature, solar irradiance, wind speed, dew point temperature, and precipitation. Meteorological data were obtained from an Arizona Meteorological Network (AZMET; http://ag.arizona.edu/azmet/) station approximately 1.5 km from the field site.

Water deficits in the CSM are simulated when the potential demand for water lost through plant transpiration and soil water evaporation is higher than the amount of water that can be supplied by the soil through the root system (Anothai et al. 2013). As in the study by Thorp et al. (2014b), potential ET was calculated using a new approach that combined the American Society of Civil Engineers (ASCE) Standardized Reference Evapotranspiration Equation (Walter et al. 2005) with the approach of DeJonge et al. (2012) for calculation of a crop coefficient from simulated LAI. The soil water balance in the CSM uses a tipping bucket approach for a one-dimensional soil profile (Ritchie 1998). The CSM also includes algorithms for soil and plant nitrogen balance simulations (Godwin and Singh 1998). Additional details about CSM-CROPGRO-Cotton can be found in Jones et al. (2003) and Thorp et al. (2014a, b).

Model inversion

Preliminary simulations showed that site-specific parameter adjustments were required to improve agreement between measured and simulated site-specific data. The simulated annealing optimization algorithm within the Geospatial Simulation tool was used for these parameter adjustments. Five model parameters were identified for adjustment between a range of values: SLAVR, RHGT, SRGF, XFRT, and EORATIO (Table 1). These parameters were selected based on prior knowledge of parameter sensitivity (Thorp et al. 2014b) and the results of preliminary optimizations that tested a variety of parameter combinations. SLAVR is the potential specific leaf area for the cultivar ($cm^2\ g^{-1}$). Preliminary optimization tests led to different ranges for SLAVR in 2009 and 2011. Thus, the upper and lower bounds for SLAVR were specified differently in the 2 years (Table 1). Higher SLAVR values in 2009 could be related to the atypical planting density in that year. RHGT is an ecotype parameter that governs the height per node relative to the standard species definition. SRGF are the root growth factors, ranging from 0 to 1, defined uniquely at each simulated soil depth increment. XFRT is the maximum fraction of daily growth that is partitioned to bolls during the reproductive growth phase. EORATIO is a maximum crop coefficient parameter used to calculate potential ET (PET) from ET_o:

$$K_c = 0.35 + (\text{EORATIO} - 0.35) * (1 - \exp(-0.70 * \text{LAI})) \quad (5)$$

$$\text{PET} = K_c * ET_o \quad (6)$$

Equation 5 was adapted from DeJonge et al. (2012) using a minimum cotton crop coefficient of 0.35 (Allen et al. 1998) and hard-coded in the model's ET routine.

Using an approach similar to Paz et al. (1998), SRGF parameters were set to 1.0 for soil layers above 30 cm and declined linearly to 0.0 below 30 cm. In this case, the parameter to

Table 1 Lower bounds (LB) and upper bounds (UB) for five model parameters adjusted by simulating annealing optimization using data from the 2009 and 2011 growing seasons

	2009		2011	
	LB	UB	LB	UB
SLAVR ($cm^2\ g^{-1}$)	130.0	230.0	90.0	190.0
RHGT	0.50	0.90	0.50	0.90
SRGF0 (cm)	150.0	350.0	150.0	350.0
XFRT	0.50	1.00	0.5	1.00
EORATIO	1.00	1.45	1.00	1.55

be optimized was the soil profile depth at which SRGF became 0.0 (SRGF0), and SRGF values in each soil layer were calculated accordingly prior to simulation. The SRGF0 parameter was permitted flexibility from 150 to 350 cm (Table 1), although the soil profile depth was simulated only to 210 cm. Thus, if SRGF0 was higher than 210 cm, the only effect was to increase SRGF parameters in all soil depths from 30 to 210 cm. The SRGF parameter for a given soil layer specifies the ability that layer to support root growth, but actual root growth and maximum simulated rooting depth also depends on photosynthate availability, soil water and nitrogen availability, and plant senescence. Specifying SRGF values in deep soil layers does not guarantee that root growth will be simulated there.

A multiple criteria objective function (f_{OBJ}) was developed to solve the inverse problem for each harvest zone in each growing season:

$$f_{\mathrm{OBJ}}=\sqrt{\sum_{i=1}^{n}\left(\alpha_i(S_i-M_i)^2\right)} \tag{7}$$

where n criteria were evaluated, S_i and M_i were respectively the simulated and measured values for the ith criterion, and α_i is a factor used to rescale data for the ith criterion. For the 2009 season, five criteria were included in the objective function, including cumulative ET from 26 May (DOY 146) to 23 September (DOY 266), maximum crop height, LAI on 3 June (DOY 154), LAI on 30 July (DOY 211), and seed cotton yield. In 2011, eight criteria were evaluated, including cumulative ET from 11 May (DOY 131) to 19 September (DOY 262), maximum crop height, seed cotton yield, and LAI on five dates: 26 May (DOY 146), 9 June (DOY 160), 21 July (DOY 202), 4 August (DOY 216), and 18 August (DOY 230). To improve the performance of the optimization, the rescaling factor, α, for each quantity was calculated as the inverse of the mean measured value and used to adjust the data to similar magnitude, typically ranging from 0 to 10. Simulated annealing optimization was set to perform a maximum of 1000 evaluations for each simulation zone with a convergence criterion of $f_{\mathrm{OBS}} < 0.05$.

The utility of the above model inversion protocol for applications in precision agriculture depends on the intended use for the model. For example, models are often used to study the results of agronomic experiments post hoc, as was true for the present study, with intent to improve model design, gain insights on model parameterization, or develop new techniques for model use. One advantage of this approach is the availability of data collected over the entire growing season, including yield. Other potential uses include guiding management decisions during the growing season or projecting future crop yield given information to date. A common issue in these modeling applications is a lack of information to characterize future conditions. For example, if the model is to be used to forecast yield, the optimization strategy tested above will not work due to lack of knowledge on future yield, which drives the adjustment of the XFRT parameter. To consider the case of within-season modeling applications, spatial optimizations were rerun while maintaining XFRT at a constant value of 0.90 and removing measured and simulated yield data from the objective function (Eq. 7). The constant XFRT value of 0.90 was based on model inversion results for XFRT with yield data included. Finally, to evaluate the model's ability without spatial optimization, simulations were rerun using the average optimized values for EORATIO, RHGT, SLAVR, SRGF, and XFRT, specified equally for all 320 harvest zones.

Successful inversion of simulation models requires the consideration of two modeling concepts: parameter identifiability and equifinality (Luo et al. 2009). Identifiable model parameters are those that can be constrained by a set of data according to a given model

formulation. Equifinality occurs when the objective function (Eq. 7) is unresponsive to parameter adjustments, resulting in multiple parameter values that fit the data equally well. To address these concepts for the present problem, model inversions with yield data included were conducted a second time using identical input data and simulation methodologies. With differences driven by the pseudorandom nature of the simulated annealing optimization algorithm, comparisons of parameter estimates from two independent model inversions provided insights on parameter identifiability and equifinality issues.

Model application

After calibrating the model for site-specific conditions, additional simulations were conducted to assess site-specific yield responses to alternative irrigation management strategies. Irrigation rates were adjusted from 50 to 130 % of the actual irrigation rates applied to each zone (i.e., the 100 % level was the same rate as actually applied.). With an incremental adjustment of 1 %, 81 alternative irrigation rates were tested. Each adjustment percentage was applied uniformly to all irrigation events during the growing season. The dates of irrigation events were not modified. Simulated seed cotton yield and total seasonal applied irrigation rate were used to calculate the irrigation water use efficiency (IWUE, kg ha^{-1} mm^{-1}) for each management alternative:

$$\text{IWUE} = \frac{\text{Seed cotton yield}}{\text{Applied irrigation depth}} \tag{8}$$

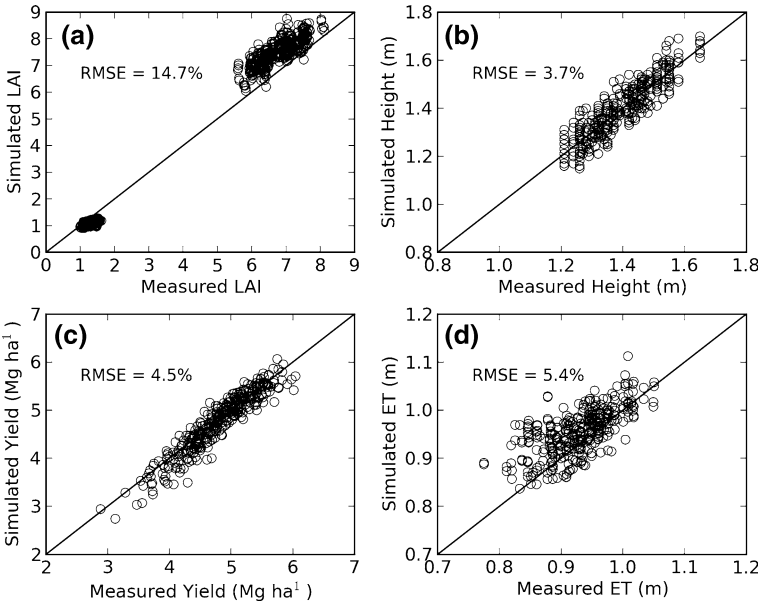

Fig. 2 Simulated versus measured **a** leaf area index (LAI) on two dates, **b** maximum cotton canopy height, **c** seed cotton yield, and **d** cumulative evapotranspiration (ET) during the 2009 growing season at Maricopa, Arizona

The simulations were used to determine the irrigation rate that maximized IWUE in each zone for both the 2009 and 2011 growing seasons. The optimum simulated irrigation rate was expressed as a percentage of the actual irrigation rate applied in each zone.

Results and discussion

Model evaluation

With site-specific optimization using a multiple criteria objective function, the model was able to simulate site-specific LAI, maximum canopy height, seed cotton yield, and seasonal ET with reasonable accuracy. For the 2009 season, the root mean squared error (RMSE) between measured and simulated data was 0.60 for LAI (14.7 % of mean observed values), 0.05 m for canopy height (3.7 % of mean observed values), 0.22 Mg ha^{-1} for yield (4.5 % of mean observed values), and 0.05 m for ET (5.4 % of mean observed values) (Fig. 2). Even after optimization, the model tended to overestimate LAI later in the growing season (Fig. 2a). The 2009 season was characterized by a higher than normal planting density, 22.0 plants m^{-2}. Since CSM-CROPGRO-Cotton was previously shown to overestimate LAI when planting densities were at this level (Thorp et al. 2014b), the model's simulation of resource competition at higher planting densities needs to be fine-tuned. Higher planting densities likely increased competition for light resources in the canopy, which led to greater stem elongation and higher measured canopy heights in 2009 (Fig. 2b) as compared to 2011 (Fig. 3b). With iterative adjustment to five parameters, the results show that the model was able to simulate spatial variability in multiple variables simultaneously.

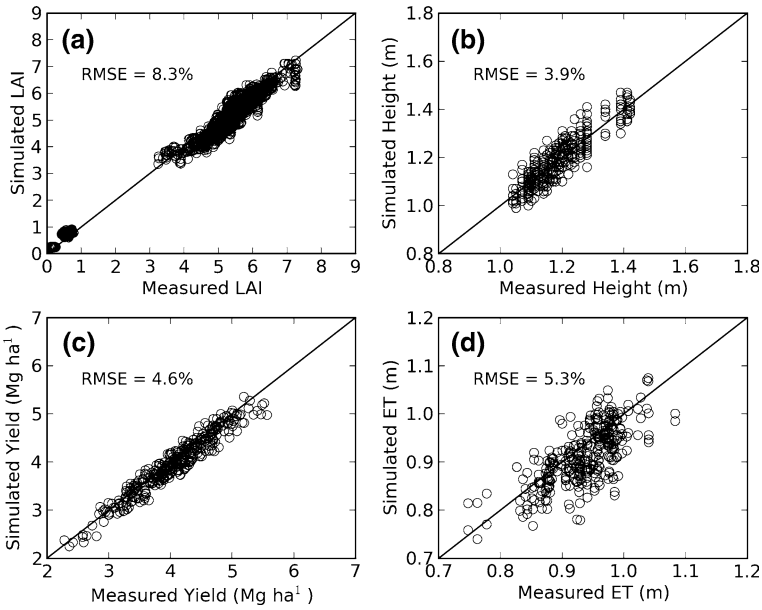

Fig. 3 Simulated versus measured **a** leaf area index (LAI) on five dates, **b** maximum cotton canopy height, **c** seed cotton yield, and **d** cumulative evapotranspiration (ET) during the 2011 growing season at Maricopa, Arizona

For the 2011 season, the RMSE between measured and simulated data was 0.28 for LAI (8.3 % of mean observed values), 0.05 m for canopy height (3.9 % of mean observed values), 0.19 Mg ha^{-1} for yield (4.6 % of mean observed values), and 0.05 m for ET (5.3 % of mean observed values) (Fig. 3). Simulations of LAI were improved in 2011 when planting density was more typical, 15.2 plants m^{-2}. Also, five observations of LAI were available in this season, which may have improved the performance of the LAI optimization as compared to 2009. It is remarkable that simulated LAI compares so well with measurements both over space and at multiple time points (Fig. 3a). Simulation errors for canopy height, seed cotton yield, and ET were similar among the 2009 and 2011 growing seasons.

Model inversion evaluation

Table 2 compares the simulation results when model inversion was tested with yield data included and yield data excluded and also when no spatial optimization was used. When spatial yield measurements were incorporated into the optimization, the model was able to collectively explain variability in measured spatial LAI, crop height, yield, and ET data (Figs. 1, 2; Table 2). Generally, RMSEs between measured and simulated values were less than 10 %, and the Pearson correlation coefficients (r) were greater than 0.70 (Table 2). Exceptions included LAI in the early season, likely due to the low magnitude of these values as compared to the potential for measurement and modeling error. Also, with yield data included, correlation coefficients for measured and simulated ET were lower (0.67 in

Table 2 Root mean squared error (RMSE) and Pearson's correlation coefficient (r) between measured and simulated data with model inversion based on inclusion and exclusion of yield data and with no spatial optimization applied

	Yield data included		Yield data excluded		No spatial optimization	
	RMSE (%)	r	RMSE (%)	r	RMSE (%)	r
2009 season						
LAI DOY 154	18.0	0.56	13.8	0.64	18.6	−0.04
LAI DOY 211	12.0	0.82	10.3	0.84	14.4	0.49
Crop Height	3.7	0.90	3.5	0.91	7.0	0.43
Yield	4.5	0.94	48.8	0.11	15.5	0.16
ET	5.4	0.67	6.2	0.75	6.2	0.59
2011 season						
LAI DOY 146	64.2	0.18	64.8	0.25	64.8	−0.07
LAI DOY 160	30.0	0.44	31.0	0.51	30.5	−0.09
LAI DOY 202	9.1	0.88	8.3	0.88	13.3	0.13
LAI DOY 216	4.3	0.95	4.0	0.96	9.1	0.02
LAI DOY 230	5.6	0.85	6.0	0.86	9.5	0.04
Crop height	3.9	0.90	2.3	0.96	7.9	0.12
Yield	4.6	0.97	26.9	0.09	16.4	0.31
ET	5.3	0.71	2.4	0.92	4.9	0.70

DOY day of year, *ET* evapotranspiration, *LAI* leaf area index

2009 and 0.71 in 2011) than that for many other variables, although RMSE was reasonable. This result highlighted several possible issues: (1) difficulty in simulating ET accurately even with model optimization, (2) greater ET variability at the scale of the 320 harvest zones than was determined at the 112 neutron access locations, and (3) uncertainty in site-specific irrigation depth estimates contributing to error in 'measured' ET estimates (Eq. 1). Optimizations with yield included represent the best fit that could be achieved with full season data given potential for both measurement and modeling error.

When yield data was excluded from the model inversion, the results demonstrated much greater RMSE between measured and simulated yield, and correlation coefficients were poor (0.11 in 2009 and 0.09 in 2011; Table 2). Generally, simulations of other variables improved due to fewer constraints on the optimization. With regard to model use for site-specific yield forecasting, these results were unfavorable and highlighted several possible issues: (1) processes that contribute to boll formation and growth in response to site-specific conditions were not adequately represented in the model, (2) the measured LAI, crop height, and ET data available in this study were insufficient to forecast crop yield using the model optimization protocol, (3) the model was overfit to measured LAI, crop height, and ET data at the expense of accurate yield simulations, and (4) the optimization should possibly focus on an alternative set of parameters. The RMSE between measured and simulated yield was greater in 2009 (48.8 %) than in 2011 (26.9 %), indicating that the additional LAI measurements in 2011 may have helped constrain the yield simulation in the latter year. Yield is perhaps the most complex yet most important trait of many field crops. Challenges to its accurate prediction using in-season data remain (Nearing et al. 2012; Thorp et al. 2010).

The results show that the model inversion approach could be practical as a guide for in-season management decisions. By removing yield from the optimization, simulations of LAI, crop height, and ET were improved in most cases (Table 2). Thus, a plausible scenario may be to use sequential estimates of LAI from remote or proximal sensors along with sequential estimates of ET from soil moisture sensors or canopy temperature sensors to update the model during the growing season. In this case, the model's utility lies in projecting LAI, biomass growth, or crop water use over a period of days or weeks until the next irrigation or fertilization event. The modeling objective would be to appropriately balance near-term crop growth with near-term resource use given economic or environmental constraints. Yield estimates would not be necessary for these decisions, especially considering that yield formation processes are not simulated until midway through the season and that management for adequate biomass accumulation is the first step to optimize yield. Alternatively, novel sensors for counting bolls could be developed to provide data for updating model parameters associated with the formation of yield components. A variety of approaches are available for such model updates, including parameter estimation approaches as described herein and also Bayesian techniques using ensemble Kalman filters (Nearing et al. 2012), although many existing crop simulation models are not well-designed for the latter approach.

Results demonstrated the importance of in-season site-specific measurements of LAI, canopy height, and ET to guide the model toward more accurate simulations of spatial variability. When the average optimized values for EORATIO, RHGT, SLAVR, SRGF, and XFRT were specified equally for all 320 harvest zones, performance statistics were generally poorer as compared to cases with spatial model optimization (Table 2). The results reflect the ability of the model to simulate spatial variability on its own, with soil hydraulic conductivity, soil water limits, bulk density, initial soil water content, and irrigation rates specified site-specifically as measured during the experiments. Perhaps with

the exception of yield, RMSEs between measured and simulated values were generally comparable, albeit higher, to the cases with spatial optimization, likely due to the model's general ability to simulate field-average conditions without spatial optimization. However, correlation coefficients were markedly reduced for many variables in both seasons. This lack of correlation between measured and simulated values demonstrates the model's inability to simulate site-specific conditions without efforts to tune model parameters using in-season measurements. Interestingly, yield simulations with no spatial optimization were better than with spatial optimization when yield was excluded. This may highlight model overfitting to other measurements as a primary reason for poor yield simulations in the latter case. Given the need for techniques to tune CSM-CROPGRO-Cotton to site-specific conditions, this study presents an approach for fitting the model to multiple site-specific measurements.

Parameter estimation

With a few exceptions, the parameters values resulting from model inversion over 320 spatial zones were normally distributed in 2009 (Fig. 4) and 2011 (Fig. 5). The SLAVR parameter (potential specific leaf area) ranged from 143 to 225 $cm^2\ g^{-1}$ with a mean of 186 $cm^2\ g^{-1}$ in 2009 (Fig. 4a) and from 106 to 176 $cm^2\ g^{-1}$ with a mean of 139 $cm^2\ g^{-1}$ in 2011 (Fig. 5a). Lower estimated values in 2011 were the result of lower maximum measured LAI in 2011 (Fig. 3a) as compared to 2009 (Fig. 2a), perhaps caused by differences in planting density. Optimized SLAVR parameter values were generally highly

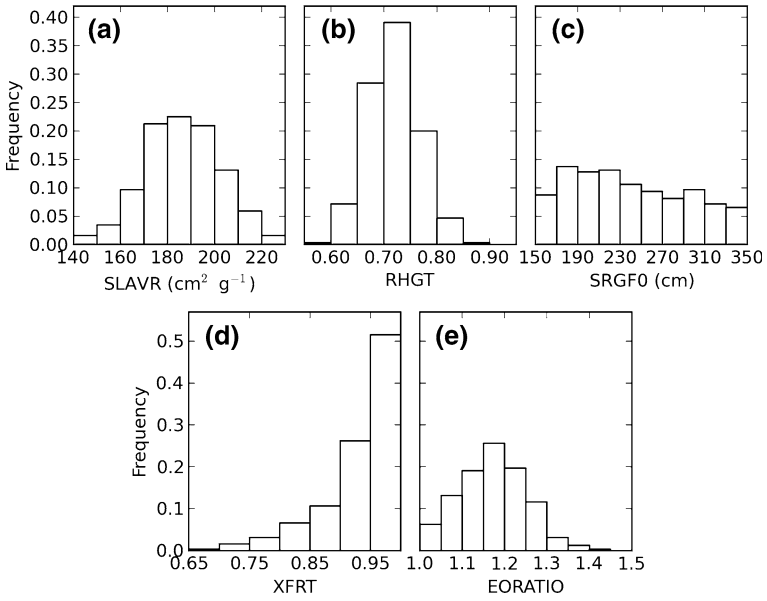

Fig. 4 Histograms of CSM-CROPGRO-Cotton parameter values resulting from simulated annealing optimization in 320 site-specific zones using data from the 2009 cotton season at Maricopa, Arizona. Optimized parameters included **a** potential specific leaf area (SLAVR), **b** relative canopy height (RHGT), **c** soil profile depth for soil root growth factor (SRGF) calculations, **d** maximum fraction of daily growth partitioned to bolls (XFRT), and **e** the maximum crop coefficient (EORATIO) for calculation of potential evapotranspiration

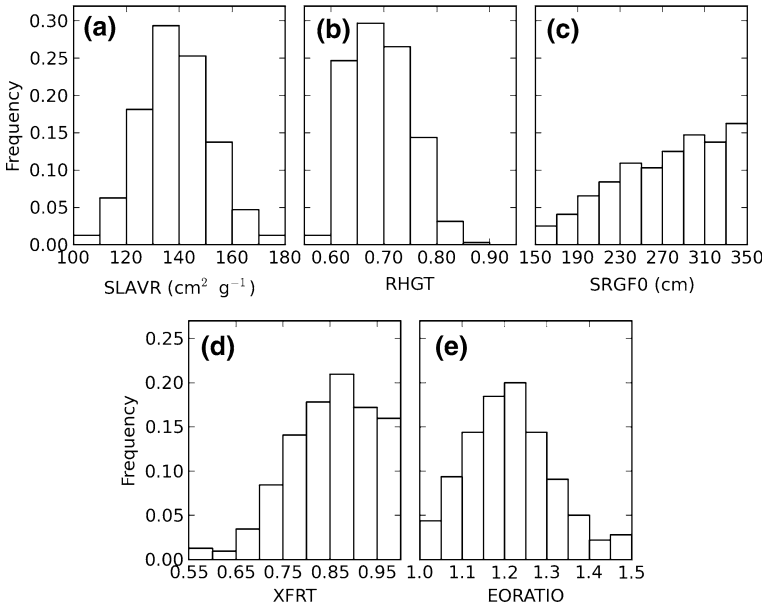

Fig. 5 Histograms of CSM-CROPGRO-Cotton parameter values resulting from simulated annealing optimization in 320 site-specific zones using data from the 2011 cotton season at Maricopa, Arizona. Optimized parameters included **a** potential specific leaf area (SLAVR), **b** relative canopy height (RHGT), **c** soil profile depth for soil root growth factor (SRGF) calculations, **d** maximum fraction of daily growth partitioned to bolls (XFRT), and **e** the maximum crop coefficient (EORATIO) for calculation of potential evapotranspiration

Table 3 Pearson's correlation coefficients (r) between optimized parameter values (SLAVR, RHGT, SRGF0, XFRT, and EORATIO) and model outputs for leaf area index (LAI) on various days of year (DOY), canopy height, seed cotton yield, and evapotranspiration (ET)

	SLAVR	RHGT	SRGF0	XFRT	EORATIO
2009 season					
LAI DOY 154	0.92	0.33	−0.10	0.27	0.10
LAI DOY 211	0.73	0.21	−0.09	−0.03	−0.17
Canopy height	0.35	0.78	−0.10	−0.12	−0.14
Yield	−0.28	−0.23	0.31	−0.06	−0.50
ET	0.15	0.07	0.22	0.30	0.87
2011 season					
LAI DOY 146	0.91	0.56	0.12	0.40	−0.18
LAI DOY 160	0.98	0.66	0.14	0.37	−0.21
LAI DOY 202	0.99	0.68	0.14	0.32	−0.23
LAI DOY 216	0.96	0.67	0.13	0.12	−0.30
LAI DOY 230	0.86	0.61	0.13	−0.16	−0.38
Canopy height	0.61	0.96	0.21	−0.10	−0.36
Yield	0.43	0.27	0.20	0.66	−0.14
ET	0.11	−0.05	−0.07	0.34	0.91

DOY day of year, *ET* evapotranspiration, *LAI* leaf area index

correlated with simulated LAI ($r > 0.9$; Table 3), indicating that the observed LAI data was mainly responsible for driving SLAVR adjustments. In 2011, SLAVR was also moderately correlated with simulated crop height ($r = 0.61$) and simulated seed cotton

yield ($r = 0.43$). Results for the RHGT parameter (relative canopy height) were similar in both seasons and ranged from 0.58 to 0.86 with a mean of 0.71 (Figs. 4b, 5b). As expected, optimum RHGT values were most highly correlated with simulated crop height ($r = 0.78$ in 2009 and $r = 0.96$ in 2011; Table 3), indicating that the observed canopy height data drove RHGT adjustments. However, RHGT was also well correlated with simulated LAI, likely because canopy height was used to calculate the LAI 'measurements' (Eq. 4). The SRGF0 parameter used to calculate the linear decline of SRGF (soil root growth factors) in each soil layer varied from 150 to 350 cm, but the distribution was non-normal in both seasons (Figs. 4c, 5c). As demonstrated by the histograms, the parameter values were on average lower in 2009 (240 cm) as compared to 2011 (275 cm). Optimized values were weakly correlated with simulated seed cotton yield ($r = 0.31$) and ET ($r = 0.22$) in 2009 and with simulated crop height ($r = 0.21$) and seed cotton yield ($r = 0.20$) in 2011 (Table 3). Mean values for the XFRT parameter (fraction of daily growth partitioned to bolls) were 0.93 in 2009 and 0.85 in 2011 (Figs. 4d, 5d). In 2009, XFRT was weakly correlated with simulated ET ($r = 0.30$), but the correlation with simulated seed cotton yield was poor ($r = -0.06$; Table 3). The tendency of XFRT values to be near the theoretical maximum of 1.0 (Fig. 4d) likely impacted the 2009 correlations. In 2011, XFRT was more highly correlated with simulated seed cotton yield ($r = 0.66$; Table 3), indicating that the observed yield data drove adjustments of XFRT in this growing season. The EORATIO parameter (maximum crop coefficient) ranged from 1.01 to 1.41 with a mean of 1.17 in 2009 (Fig. 4e) and from 1.00 to 1.50 with a mean of 1.21 in 2011 (Fig. 5e). The EORATIO values were highly correlated with simulated ET ($r = 0.87$ in 2009 and $r = 0.91$ in 2011; Table 3), indicating as expected that the observed ET data drove

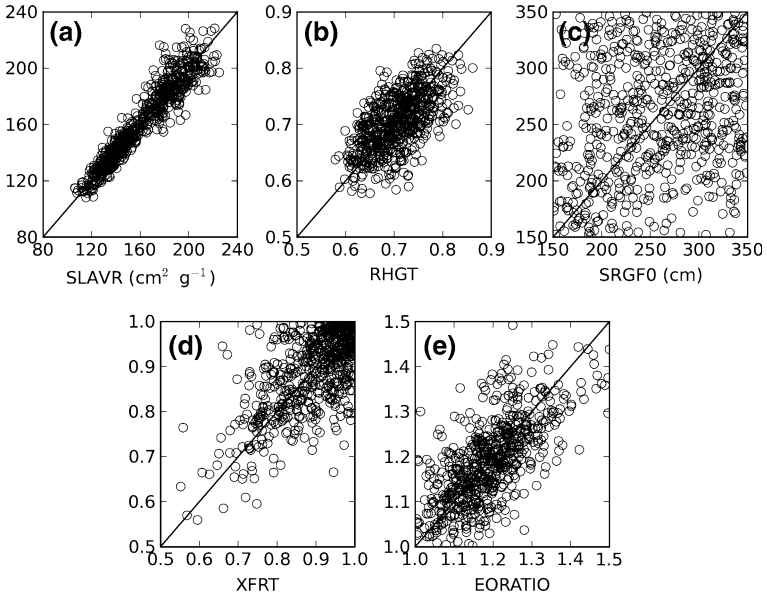

Fig. 6 Comparison of optimal parameter values from two model inversions based on identical input data. Results are shown for **a** potential specific leaf area (SLAVR), **b** relative canopy height (RHGT), **c** soil profile depth for soil root growth factor (SRGF) calculations, **d** maximum fraction of daily growth partitioned to bolls (XFRT), and **e** the maximum crop coefficient (EORATIO). Data are compared for 320 management zones in both the 2009 and 2011 growing seasons at Maricopa, Arizona

adjustments of EORATIO. Correlation results demonstrated that the optimum parameter values were differentially impacted by the measurements incorporated in the multiple criteria objective function (Table 3).

Parameter identifiability and equifinality evaluation

Comparing the resulting SLAVR values from two independent model inversions showed that the SLAVR estimates were highly repeatable (Fig. 6a). As compared to other optimized parameters, SLAVR values from independent model inversions had lower RMSE and were more highly correlated (Table 4). This means SLAVR demonstrated relatively good parameter identifiability and did not lead to equifinality of the model's response surface. With better performance statistics in 2011 as compared to 2009, the SLAVR parameter was more identifiable in 2011, likely due to more LAI measurements in that year. Comparisons of the SRGF0 parameter values demonstrated obvious problems (Fig. 6c). The optimum values for this parameter were often dissimilar when comparing two independent model inversions, and RMSE and correlation statistics were worst among all the parameters (Table 4). The model inversion procedure was less able to identify this parameter given the available data, and the objective function was likely unresponsive to adjustments of this parameter, especially as compared to the other parameters. As a result, the semi-random nature of the simulated annealing algorithm led to large discrepancies in the optimal SRGF0 values obtained from independent optimizations. One positive outcome was that the correlations of the SRGF0 parameter with simulated yield from the second model inversion (Table 4) was very similar to that result for the first model inversion (Table 3). Although these correlations were weak, they were consistent for two model inversions in both growing seasons. Thus, the adjustment of SRGF provided at least minimal guidance for improvements in the simulation of spatial yield, as previously demonstrated by Paz et al. (1998). Due to great uncertainty about the dynamics of root growth and difficulties in constraining SRGF parameters without such knowledge, continued investigation into methods for adjustments of the root growth simulation is recommended. For example, instead of using a linear decline in SRGF with soil profile depth, alternative shape functions could be tested.

The RMSEs between measured and simulated LAI, canopy height, seed cotton yield, and ET from the second model inversion (not shown) were all within 0.4 % of that obtained for the first model inversion (Figs. 2, 3). Plots of these relationships were also not visually different. Thus, although estimates from two model inversions varied substantially for some parameters (Fig. 6), the resulting simulation outcome was essentially the same. This highlights the equifinality issues in this model inversion problem.

Table 4 Root mean squared error (RMSE) and Pearson's correlation coefficient (r) between optimal parameter values from two independent model inversions based on identical input data and simulation methodologies

	SLAVR	RHGT	SRGF0	XFRT	EORATIO
2009 RMSE (%)	6.0	6.8	29.0	7.9	5.3
2009 r	0.75	0.47	0.17	0.37	0.68
2011 RMSE (%)	3.9	5.8	23.0	8.7	7.1
2011 r	0.92	0.72	0.20	0.68	0.65

Irrigation analysis

Simulations of the irrigation rate that maximized IWUE in each zone permitted evaluation of the four irrigation scheduling approaches used during the field experiment. Averaged over zones, the simulated seasonal deep seepage rates with the applied irrigation rates in 2009 were 4, 59, 37, and 34 mm for the FAO, MAC, VI_A, and VI_B treatments, respectively. Also, the optimum simulated irrigation rates for FAO, MAC, VI_A, and VI_B treatments were 111, 92, 98, and 96 %, respectively, of actual irrigation rates applied in 2009 (Fig. 7). Thus, the MAC treatment generally received too much irrigation, because deep seepage was highest among all treatments and only 92 % of the actual irrigation rate was needed to optimize simulated IWUE. On the other hand, the FAO treatment received too little irrigation, because the simulation analysis showed that 111 % of the actual irrigation rate was needed to optimize simulated IWUE. The treatments managed using NDVI from remote sensing images were only slightly over irrigated in 2009, indicating that the techniques led to improved irrigation management as compared to more traditional methods. Under irrigation by the FAO method was likely related to the high planting density in 2009, because the FAO irrigation scheduling model did not account for planting density effects on ET. The remote sensing approaches accounted for this affect using dynamic vegetation indices, while FAO did not account for it. Effects of spatially variable infiltration are evident, particularly for the FAO treatments (Fig. 7). For three of the four FAO treatments, there is evidence that the southern portion of the treatment plot received irrigation applications that more closely matched the optimum irrigation rate (i.e., values closer to 100 %), while the northern portion of the FAO plots typically needed over 110 % of actual irrigation applied to maximize simulated IWUE. This spatial pattern is likely due to increased opportunity time for infiltration on the southern side of the field, where surface irrigation commenced. The effect was stronger for FAO, because this treatment received

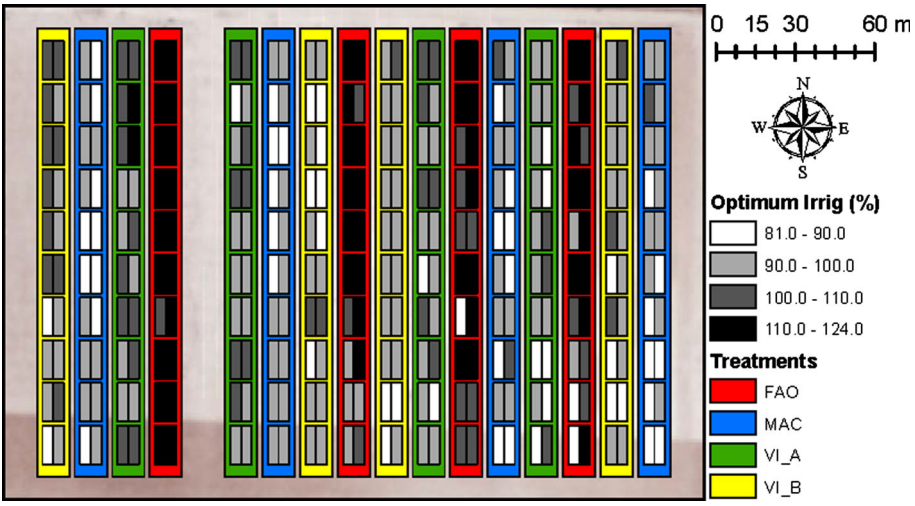

Fig. 7 Irrigation rates that maximized the simulated irrigation water use efficiency in the 2009 growing season, expressed as a percentage of actual irrigation rate applied. Simulations showed that MAC treatment plots were generally over-irrigated while FAO treatment plots were under-irrigated in 2009 (Color figure online)

the lowest irrigation rate. Increased opportunity time for infiltration on the south side of the FAO plots left the north side in a more severe water deficit condition.

In 2011, simulated cumulative deep seepage rates with the applied irrigation rates were higher than the first season: 87, 69, 104, and 80 mm for FAO, MAC, VI_A, and VI_B treatments, respectively. Irrigation rates that maximized simulated IWUE for FAO, MAC, VI_A, and VI_B treatments were 89, 96, 88, and 94 %, respectively, of actual irrigation rates applied (Fig. 8). Thus, all four of the irrigation scheduling methods generally resulted in over irrigation. The FAO method did not lead to under irrigation in 2011, because the planting density was more typical. Under-irrigated zones were more related to surface irrigation effects, particularly in the northeastern portion of the field. Independent of treatment, plots in the easternmost treatment block were more well-watered in the south central portion of the plot as compared to the northern portion of the plot. This could again be due to increased opportunity time for infiltration in the southern portion of the field, where surface irrigation commenced. However, this effect was typically not demonstrated in the westernmost treatment blocks. This could highlight an effect due to soil texture variability. Since the western portion of the field was more clayey and the eastern portion was more sandy, the eastern treatments could be more sensitive to spatially variable infiltration opportunity time, while the clay in the west helped to mitigate the issue.

One issue with this irrigation analysis was the assumption that all parameters other than irrigation rates remained fixed at the value obtained from the model inversion procedure. In reality, changing the irrigation rate in a zone would also change the measured ET from Eq. 1, which could in turn change the value obtained for EORATIO during model inversion. Likewise, real adjustments to irrigation rates would also likely impact measured LAI, canopy height, and seed cotton yield by changing water interactions, which would in turn affect values obtained for SLAVR, RHGT, and XFRT with model inversion. Results of this study demonstrated that site-specific parameter adjustments were needed to simulate spatial variability in crop growth characteristics and ET (Table 2; Figs. 4, 5). Results also

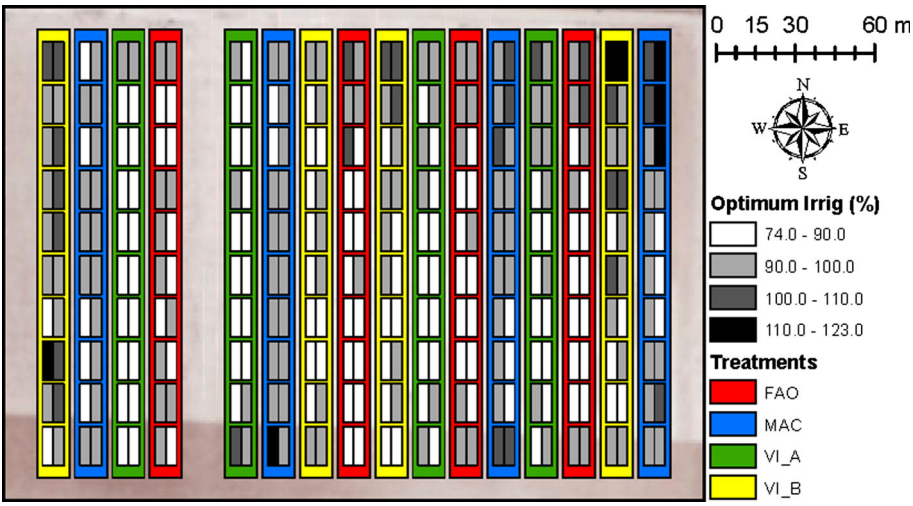

Fig. 8 Irrigation rates that maximized the simulated irrigation water use efficiency in the 2011 growing season, expressed as a percentage of actual irrigation rate applied. Simulations showed that much of the field was over-irrigated in 2011 (Color figure online)

showed that parameter estimates could vary substantially as a result of equifinality (Fig. 6), but led to the same simulation outcome. This may lead to questions on whether the estimated site-specific parameters were meaningful enough to provide realistic simulated seed cotton yield and IWUE responses to irrigation rate adjustments. The conclusion was that meaning can be derived, because spatial patterns related to the irrigation scheduling method were present (Fig. 7) and spatial patterns potentially explained by the surface irrigation dynamics were evident (Figs. 7, 8). Also, several of the treatment plots were over irrigated in all 20 harvest zones (Figs. 7, 8) and one was under irrigated in all 20 zones (Fig. 7), a result that would be unexpected if random effects associated with parameter estimation were an issue.

Since surface irrigation was used for the field experiment, estimating the irrigation depths applied in each zone was perhaps the most challenging aspect of this simulation study. An in-line flow meter provided the total volume of water applied to each treatment plot, but complex hydraulic processes determined the spatial distribution of infiltration within the plot area. Spatial variability in infiltration potentially resulted from surface irrigation management factors (Hunsaker et al. 1999) and spatial variability in soil type or preferential flow paths (Jaynes and Hunsaker 1989). Additionally, an unknown quantity of water moved laterally into the surrounding border dikes during surface irrigation, which complicated the calculation of irrigation depth from measured irrigation volume and plot area. Analysis of advance and recession data and WinSRFR simulation results assisted with spatial irrigation depth specification, but considerable uncertainty in these estimates remained and likely contributed to simulation uncertainty reported in this study. Preliminary efforts aimed to reduce this uncertainty by incorporating the adjustment of irrigation rates into the model inversion protocol. However, these efforts failed, because changing irrigation rates changed estimates of measured ET (Eq. 1) which made the minimum solution of the objective function (Eq. 7) a moving target. Also, adjusting the zone-level irrigation rates required that water be redistributed spatially to maintain the water balance within a treatment plot, given the total volume of water applied. This greatly complicated the model inversion procedure, because parameters for 20 zones had to be adjusted collectively. In the end, irrigation rates were held fixed using best estimates, and other parameters were adjusted as described above. Central pivot and lateral move irrigation systems offer great potential to improve the methodologies reported herein, because applied site-specific irrigation rates could be better quantified. Also, such systems would permit field testing of the precision irrigation recommendations generated from this simulation approach.

Conclusions

An advanced goal for precision agriculture is the integration of real-time sensor data with computer algorithms to provide recommendations for variable-rate application of irrigation and nitrogen fertilizer while considering potential environmental impacts, resource limitations, and climate forecasts. This requires the development of both hardware and software components and techniques to integrate them. Advancing toward this goal, the present study synthesized information from multiple sources to adjust the CSM-CROPGRO-Cotton model to site-specific crop and water use conditions. Positive methodological outcomes included (1) further testing of the Geospatial Simulation software (Thorp and Bronson 2013) to integrate multiple geospatial data sets and conduct simulation analyses

for two cotton experiments in Arizona, (2) the identification of several sensitive parameters for fitting the CSM-CROPGRO-Cotton model to site-specific data, and (3) the development of a methodology to optimize the model using multiple criteria objective functions. The approach led to satisfactory comparisons of measured and simulated data for both cotton growing seasons, although assessments of parameter identifiability and equifinality suggested that parameter estimates were sometimes non-unique. Some parameters were more identifiable than others, and identifiability depended on the data available for model inversion. Future investigation should identify ways to mitigate these effects, for example through modification of the simulation algorithm, refinement of the model inversion strategy, or inclusion of additional data sets.

Efforts to use the simulation methodology for real-time precision irrigation management would identify bottlenecks in data collection and processing pipelines and improve the reliability of the approach for practical on-farm use. The present study aimed to integrate data from multiple sources to characterize different aspects of the cropping system, but there remains great opportunity for streamlining the platforms and procedures used to collect these data. For example, active reflectance sensors mounted on ground-based vehicles are an alternative to passive airborne imaging. Also, ultrasonic sensors are being developed for plant height measurements (Scotford and Miller 2004), which would eliminate reliance on manual approaches. Incorporating reflectance sensors, ultrasonic sensors, and soil moisture sensors into a wireless sensor network would provide all the data needed for real-time, site-specific analysis of crop responses to irrigation management using the simulation methodology presented herein. Unmanned aerial vehicles are another potential platform for airborne data, but the need for soil moisture and plant height measurements favors data collection approaches on the ground. The Geospatial Simulation software was designed to streamline geospatial data processing and integration, but data from some sources, images for example, can require additional processing outside of the GIS environment. The present study provides guidance on the types of data that are necessary, but the best approach to collect these data remains unclear and likely depends on the specific application.

Once the appropriate data can be rapidly collected and integrated with appropriate computer algorithms, the benefits of precision crop management can be realized. After calibration to site-specific conditions, CSM-CROPGRO-Cotton identified areas of the field that required more or less irrigation water to maximize simulated IWUE. For operational capability, future research should reduce the computational time for simulations, perhaps by simplifying the algorithm to include only the processes necessary for irrigation management or by investigating options for parallelization on multi-core processors. This study demonstrated the strength of models that combine simulations of both crop growth and soil water balance, which facilitated the synthesis of data from multiple sources and permitted calculations of IWUE as a statistic for optimizing site-specific irrigation management.

References

Allen, R. G., Pereira, L. S., Raes, D., & Smith. M. (1998). Crop evapotranspiration—Guidelines for computing crop water requirements—FAO Irrigation and Drainage Paper 56. Food and Agriculture Organization of the United Nations, Rome, Italy. Available online at http://www.fao.org/docrep/x0490e/x0490e00.HTM. Accessed 22 May 2014.

Anothai, J., Soler, C. M. T., Green, A., Trout, T. J., & Hoogenboom, G. (2013). Evaluation of two evapotranspiration approaches simulated with the CSM-CERES-Maize model under different

irrigation strategies and the impact on maize growth, development, and soil moisture content for semi-arid conditions. *Agricultural and Forest Meteorology, 176*(1), 64–76.

Baumhardt, R. L., Staggenborg, S. A., Gowda, P. H., Colaizzi, P. D., & Howell, T. A. (2009). Modeling irrigation management strategies to maximize cotton lint yield and water use efficiency. *Agronomy Journal, 101*(3), 460–468.

Bautista, E., Clemmens, A. J., Strelkoff, T. S., & Schlegel, J. (2009). Modern analysis of surface irrigation systems with WinSRFR. *Agricultural Water Management, 96*(7), 1146–1154.

Boote, K. J., & Pickering, N. B. (1994). Modeling photosynthesis of row crop canopies. *HortScience, 29*(12), 1423–1434.

Calmon, M. A., Jones, J. W., Shinde, D., & Specht, J. E. (1999). Estimating parameters for soil water balance models using adaptive simulated annealing. *Applied Engineering in Agriculture, 15*(6), 703–713.

Cammarano, D., Payero, J., Basso, B., Wilkens, P., & Grace, P. (2012). Agronomic and economic evaluation of irrigation strategies on cotton lint yield in Australia. *Crop & Pasture Science, 63*(7), 647–655.

Camp, C. R., Sadler, E. J., Evans, D. E., Usrey, L. J., & Omary, M. (1998). Modified center pivot system for precision management of water and nutrients. *Applied Engineering in Agriculture, 14*(1), 23–31.

Charoenhirunyingyos, S., Honda, K., Kamthonkiat, D., & Ines, A. V. M. (2011). Soil moisture estimation from inverse modeling using multiple criteria functions. *Computers and Electronics in Agriculture, 75*(2), 278–287.

Chávez, J. L., Pierce, F. J., Elliott, T. V., & Evans, R. G. (2010). A remote irrigation monitoring and control system for continuous move systems. Part A: description and development. *Precision Agriculture, 11*(1), 1–10.

DeJonge, K. C., Ascough, J. C, I. I., Andales, A. A., Hansen, N. C., Garcia, L. A., & Arabi, M. (2012). Improving evapotranspiration simulations in the CERES-Maize model under limited irrigation. *Agricultural Water Management, 115*, 92–103.

DeJonge, K. C., Kaleita, A. L., & Thorp, K. R. (2007). Simulating the effects of spatially variable irrigation on corn yields, costs, and revenue in Iowa. *Agricultural Water Management, 92*(1–2), 99–109.

El Nahry, A. H., Ali, R. R., & El Baroudy, A. A. (2011). An approach for precision farming under pivot irrigation system using remote sensing and GIS techniques. *Agricultural Water Management, 98*(4), 517–531.

Evans, R. G., & King, B. A. (2012). Site-specific sprinkler irrigation in a water-limited future. *Transactions of the ASABE, 55*(2), 493–504.

Farquhar, G. D., Von Caemmerer, S., & Berry, J. A. (1980). A biochemical model of photosynthetic CO_2 assimilation in leaves of C_3 species. *Planta, 149*(1), 78–90.

French, A. N., Hunsaker, D. J., & Thorp, K. R. (2015). Remote sensing of evapotranspiration over cotton using the TSEB and METRIC energy balance models. *Remote Sensing of Environment, 158*, 281–294.

Gee, G. W., & Bauder, J. W. (1986). Particle-size analysis. In A. Klute (Ed.), *Methods of soil analysis, Part I*. Madison: American Society of Agronomy.

Godwin, D. C., & Singh, U. (1998). Nitrogen balance and crop response to nitrogen in upland and lowland cropping systems. In G. Y. Tsuji, G. Hoogenboom, & P. K. Thornton (Eds.), *Understanding options for agricultural production* (pp. 55–77). Dordrecht: Kluwer Academic Publishers.

Hadria, R., Duchemin, B., Lahrouni, A., Khabba, S., Er-Raki, S., Dedieu, G., et al. (2006). Monitoring of irrigated wheat in a semi-arid climate using crop modelling and remote sensing data: Impact of satellite revisit time frequency. *International Journal of Remote Sensing, 27*(5–6), 1093–1117.

Heinemann, A. B., Hoogenboom, G., & De Faria, R. T. (2002). Determination of spatial water requirements at county and regional levels using crop models and GIS: An example for the State of Parana, Brazil. *Agricultural Water Management, 52*(3), 177–196.

Hood, C. P., McClendon, R. W., & Hook, J. E. (1987). Computer analysis of soybean irrigation management strategies. *Transactions of the ASAE, 30*(2), 417–423.

Hoogenboom, G., Jones, J. W., Wilkens, P. W., Porter, C. H., Boote, K. J., Hunt, L. A., Singh, U., Lizaso, J. L., White, J. W., Uryasev, O., Royce, F. S., Ogoshi, R., Gijsman, A. J., Tsuji, G. Y., & Koo, J. (2012). Decision support system for agrotechnology transfer (DSSAT). Version 4.5.1.005 [CD-ROM]. University of Hawaii, Honolulu, Hawaii.

Hook, J. E. (1994). Using crop models to plan water withdrawals for irrigation in drought years. *Agricultural Systems, 45*(3), 271–289.

Hunsaker, D. J., Barnes, E. M., Clarke, T. R., Fitzgerald, G. J., & Pinter, P. J. (2005). Cotton irrigation scheduling using remotely sensed and FAO-56 basal crop coefficients. *Transactions of the ASAE, 48*(4), 1395–1407.

Hunsaker, D. J., Clemmens, A. J., & Fangmeier, D. D. (1999). Cultural and irrigation management effects on infiltration, soil roughness, and advance in furrowed level basins. *Transactions of the ASAE, 42*(6), 1753–1762.

Hunsaker, D. J., French, A. N., Waller, P. M., Bautista, E., Thorp, K. R., & Andrade-Sanchez, P. (2015). Irrigation scheduling using spatial information in real-time: An evaluation with cotton grown under surface irrigation. Irrigation Science, in review.

Hunsaker, D. J., Pettit, D. E., & Clemmens, A. J. (2011). A self-contained probe for measuring water advance and recession times in surface-irrigated fields. *Applied Engineering in Agriculture, 27*(5), 729–736.

Ines, A. V. M., Gupta, A. D., & Loof, R. (2002). Application of GIS and crop growth models in estimating water productivity. *Agricultural Water Management, 54*(3), 205–225.

Irmak, A., Jones, J. W., Batchelor, W. D., & Paz, J. O. (2001). Estimating spatially variable soil properties for application of crop models in precision farming. *Transactions of the ASAE, 44*(5), 1343–1353.

Jaynes, D. B., & Hunsaker, D. J. (1989). Spatial and temporal variability of water content and infiltration on a flood irrigated field. *Transactions of the ASAE, 32*(4), 1229–1238.

Jones, J. W., Hoogenboom, G., Porter, C. H., Boote, K. J., Batchelor, W. D., Hunt, L. A., et al. (2003). The DSSAT cropping system model. *European Journal of Agronomy, 18*(3–4), 235–265.

Ju, W., Gao, P., Wang, J., Zhou, Y., & Zhang, X. (2010). Combining an ecological model with remote sensing and GIS techniques to monitor soil water content of croplands with a monsoon climate. *Agricultural Water Management, 97*(8), 1221–1231.

Kranz, W. L., Evans, R. G., Lamm, F. R., O'Shaughnessy, S. A., & Peters, R. T. (2012). A review of mechanical move sprinkler irrigation control and automation technologies. *Applied Engineering in Agriculture, 28*(3), 389–397.

Liu, J. (2009). A GIS-based tool for modelling large-scale crop-water relations. *Environmental Modelling and Software, 24*(3), 411–422.

Luo, Y., Weng, E., Wu, X., Gao, C., Zhou, X., & Zhang, L. (2009). Parameter identifiability, constraint, and equifinality in data assimilation with ecosystem models. *Ecological Applications, 19*(3), 571–574.

Mauget, S., Leiker, G., & Nair, S. (2013). A web application for cotton irrigation management on the U.S. Southern High Plains. Part I: Crop yield modeling and profit analysis. *Computers and Electronics in Agriculture, 99*, 248–257.

McCarthy, A. C., Hancock, N. H., & Raine, S. R. (2010). VARIwise: A general-purpose adaptive control simulation framework for spatially and temporally varied irrigation at sub-field scale. *Computers and Electronics in Agriculture, 70*(1), 117–128.

McKinion, J. M., Jenkins, J. N., Akins, D., Turner, S. B., Willers, J. L., Jallas, E., & Whisler, F. D. (2001). Analysis of a precision agriculture approach to cotton production. *Computers and Electronics in Agriculture, 32*(3), 213–228.

Mo, X., Liu, S., Lin, Z., Xu, Y., Xiang, Y., & McVicar, T. R. (2005). Prediction of crop yield, water consumption and water use efficiency with a SVAT-crop growth model using remotely sensed data on the North China Plain. *Ecological Modelling, 183*(2–3), 301–322.

Monaghan, J. M., Daccache, A., Vickers, L. H., Hess, T. M., Weatherhead, E. K., Grove, I. G., & Knox, J. W. (2013). More 'crop per drop': Constraints and opportunities for precision irrigation in European agriculture. *Journal of the Science of Food and Agriculture, 93*(5), 977–980.

Nair, S., Maas, S., Wang, C., & Mauget, S. (2013). Optimal field partitioning for center-pivot-irrigated cotton in the Texas High Plains. *Agronomy Journal, 105*(1), 124–133.

Nearing, G. S., Crow, W. T., Thorp, K. R., Moran, M. S., Reichle, R. H., & Gupta, H. V. (2012). Assimilating remote sensing observations of leaf area index and soil moisture for wheat yield estimates: An observing system simulation experiment. *Water Resources Research, 48*, W05525. doi:10.1029/2011WR011420.

Paz, J. O., Batchelor, W. D., Colvin, T. S., Logsdon, S. D., Kaspar, T. C., & Karlen, D. L. (1998). Analysis of water stress effects causing spatial yield variability in soybeans. *Transactions of the ASAE, 41*(5), 1527–1534.

Pereira, L. S., Oweis, T., & Zairi, A. (2002). Irrigation management under water scarcity. *Agricultural Water Management, 57*(3), 175–206.

Rao, M. N., Waits, D. A., & Neilsen, M. L. (2000). A GIS-based modeling approach for implementation of sustainable farm management practices. *Environmental Modelling and Software, 15*(8), 745–753.

Ritchie, J. T. (1998). Soil water balance and plant water stress. In G. Y. Tsuji, G. Hoogenboom, & P. K. Thornton (Eds.), *Understanding options for agricultural production* (pp. 41–54). Dordrecht: Kluwer Academic Publishers.

Schaap, M. G., Leij, F. J., & Van Genuchten, M. T. (2001). ROSETTA: a computer program for estimating soil hydraulic parameters with hierarchical pedotransfer functions. *Journal of Hydrology, 251*(3–4), 163–176.

Scotford, I. M., & Miller, P. C. H. (2004). Estimating tiller density and leaf area index of winter wheat using spectral reflectance and ultrasonic sensing techniques. *Biosystems Engineering, 89*(4), 395–408.

Seidl, M. S., Batchelor, W. D., & Paz, J. O. (2004). Integrating remotely sensed images with a soybean model to improve spatial yield simulation. *Transactions of the ASAE, 47*(6), 2081–2090.

Thorp, K. R., Ale, S., Bange, M. P., Barnes, E. M., Hoogenboom, G., Lascano, R. J., et al. (2014a). Development and application of process-based simulation models for cotton production: A review of past, present, and future directions. *Journal of Cotton Science, 18*(1), 1–38.

Thorp, K. R., Barnes, E. M., Hunsaker, D. J., Kimball, B. A., White, J. W., Nazareth, V. J., & Hoogenboom, G. (2014b). Evaluation of CSM-CROPGRO-Cotton for simulating effects of management and climate change on cotton growth and evapotranspiration in an arid environment. *Transactions of the ASABE, 57*(6), 1627–1642.

Thorp, K. R., Batchelor, W. D., Paz, J. O., Kaleita, A. L., & DeJonge, K. C. (2007). Using cross-validation to evaluate CERES-Maize yield simulations within a decision support system for precision agriculture. *Transactions of the ASABE, 50*(4), 1467–1479.

Thorp, K. R., Batchelor, W. D., Paz, J. O., Steward, B. L., & Caragea, P. C. (2006). Methodology to link production and environmental risks of precision nitrogen management strategies in corn. *Agricultural Systems, 89*(2–3), 272–298.

Thorp, K. R., & Bronson, K. F. (2013). A model-independent open-source geospatial tool for managing point-based environmental model simulations at multiple spatial locations. *Environmental Modelling and Software, 50*, 25–36.

Thorp, K. R., DeJonge, K. C., Kaleita, A. L., Batchelor, W. D., & Paz, J. O. (2008). Methodology for the use of DSSAT models for precision agriculture decision support. *Computers and Electronics in Agriculture, 64*(2), 276–285.

Thorp, K. R., Hunsaker, D. J., & French, A. N. (2010). Assimilating leaf area index estimates from remote sensing into the simulations of a cropping systems model. *Transactions of the ASABE, 53*(1), 251–262.

Thorp, K. R., Wang, G., West, A. L., Moran, M. S., Bronson, K. F., White, J. W., & Mon, J. (2012). Estimating crop biophysical properties from remote sensing data by inverting linked radiative transfer and ecophysiological models. *Remote Sensing of Environment, 124*, 224–233.

Walter, I. A., Allen, R. G., Elliott, R., Itenfisu, D., Brown, P., Jensen, M. E., Mecham, B., Howell, T. A., Snyder, R., Eching, S., Spofford, T., Hattendorf, M., Martin, D., Cuenca, R. H., & Wright, J. L. (2005). The ASCE Standardized Reference Evapotranspiration Equation. Final Report of the Task Committee on Standardization of Reference Evapotranspiration, Environmental and Water Resources Institute (EWRI), American Society of Civil Engineers (ASCE), Restin, Virginia. Available online at http://www.kimberly.uidaho.edu/water/asceewri/ascestzdetmain2005.pdf. Accessed 30 May 2014.

Zhang, K., Hilton, H. W., Greenwood, D. J., & Thompson, A. J. (2011). A rigorous approach of determining FAO56 dual crop coefficient using soil sensor measurements and inverse modeling techniques. *Agricultural Water Management, 98*(6), 1081–1090.